

# Magnetic levitation technique for active vibration control

Md. Emdadul Hoque and Takeshi Mizuno  
*Saitama University*  
*Japan*

## 1. Introduction

This chapter presents an application of zero-power controlled magnetic levitation for active vibration control. Vibration isolation are strongly required in the field of high-resolution measurement and micromanufacturing, for instance, in the submicron semiconductor chip manufacturing, scanning probe microscopy, holographic interferometry, cofocal optical imaging, etc. to obtain precise and repeatable results. The growing demand for tighter production tolerance and higher resolution leads to the stringent requirements in these research and industry environments. The microvibrations resulted from the tabletop and/or the ground vibration should be carefully eliminated from such sophisticated systems. The vibration control research has been advanced with passive and active techniques. Conventional passive technique uses spring and damper as isolator. They are widely used to support the investigated part to protect it from the severe ground vibration or from direct disturbance on the table by using soft and stiff suspensions, respectively (Haris & Piersol, 2002; Rivin, 2003). Soft suspensions can be used because they provide low resonance frequency of the isolation system and thus reduce the frequency band of vibration amplification. However, it leads to potential problem with static stability due to direct disturbance on the table, which can be solved by using stiff suspension. On the other hand, passive systems offer good high frequency vibration isolation with low isolator damping at the cost of vibration amplification at the fundamental resonance frequency. It can be solved by using high value of isolator damping. Therefore, the performance of passive isolators are limited, because various trade-offs are necessary when excitations with a wide frequency range are involved.

Active control technique can be introduced to resolve these drawbacks. Active control system has enhanced performances because it can adapt to changing environment (Fuller et al., 1997; Preumont, 2002; Karnopp, 1995). Although conventional active control system achieves high performance, it requires large amount of energy source to drive the actuators to produce active damping force (Benassi et al., 2004a & 2004b; Yoshioka et al., 2001; Preumont et al., 2002; Daley et al., 2006; Zhu et al., 2006; Sato & Trumper, 2002). Apart from this, most of the researches use high-performance sensors, such as servo-type accelerometer for detecting vibration signal, which are rather expensive. These are the difficulties to expand the application fields of active control technique.

The development and maintenance cost of vibration isolation system should be lowered in order to expand the application fields of active control. Considering the point of view, a vibration isolation system have been developed using an actively zero-power controlled magnetic levitation system (Hoque et al., 2006; Mizuno et al., 2007a; Hoque et al., 2010a). In the proposed system, eddy-current relative displacement sensors were used for displacement feedback. Moreover, the control current converges to zero for the zero-power control system. Therefore, the developed system becomes rather inexpensive than the conventional active systems.

An active zero-power controlled magnetic suspension is used in this chapter to realize negative stiffness by using a hybrid magnet consists of electromagnet and permanent magnets. Moreover, it can be noted that realizing negative stiffness can also be generalized by using linear actuator (voice coil motor) instead of hybrid magnet (Mizuno et al., 2007b). This control achieves the steady state in which the attractive force produced by the permanent magnets balances the weight of the suspended object, and the control current converges to zero. However, the conventional zero-power controller generates constant negative stiffness, which depends on the capacity of the permanent magnets. This is one of the bottlenecks in the field of application of zero-power control where the adjustment of stiffness is necessary. Therefore, this chapter will investigate on an improved zero-power controller that has capability to adjust negative stiffness. Apart from this, zero-power control has inherently nonlinear characteristics. However, compensation to zero-power control can solve such problems (Hoque et al., 2010b). Since there is no steady energy consumption for achieving stable levitation, it has been applied to space vehicles (Sabnis et al., 1975), to the magnetically levitated carrier system in clean rooms (Morishita et al., 1989) and to the vibration isolator (Mizuno et al., 2007a). Six-axis vibration isolation system can be developed as well using this technique (Hoque et al., 2010a).

In this chapter, an active vibration isolation system is developed using zero-power controlled magnetic levitation technology. The isolation system is fabricated by connecting a mechanical spring in series with a suspension of negative stiffness (see Section 4 for details). Middle tables are introduced in between the base and the isolation table.

In this context, the nomenclature on the vibration disturbances, compliance and transmissibility are discussed for better understanding. The underlying concept on vibration isolation using magnetic levitation technique, realization of zero-power, stiffness adjustment, nonlinear compensation of the maglev system are presented in detail. Some experimental results are presented for typical vibration isolation systems to demonstrate that the maglev technique can be implemented to develop vibration isolation system.

## 2. Vibration Suppression Terminology

### 2.1 Vibration Disturbances

The vibration disturbance sources are categorized into two groups. One is direct disturbance or tabletop vibration and another is ground or floor vibration.

*Direct disturbance* is defined by the vibrations that applies to the tabletop and generates deflection or deformation of the system. *Ground vibration* is defined by the detrimental vibrations that transmit from floor to the system through the suspension. It is worth noting that zero or low compliance for tabletop vibration and low transmissibility (less than unity) are ideal for designing a vibration isolation system.

Almost in every environment, from laboratory to industry, vibrational disturbance sources are common. In modern research or application arena, it is certainly necessary to conduct experiments or make measurements in a vibration-free environment. Think about a industry or laboratory where a number of energy sources exist simultaneously. Consider the silicon wafer photolithography system, a principal equipment in the semiconductor manufacturing process. It has a stage which moves in steps and causes disturbance on the table. It supports electric motors, that generates periodic disturbance. The floor also holds some rotating machines. Moreover, earthquake, movement of employees with trolley transmit seismic disturbance to the stage. Assume a laboratory measurement table in another case. The table supports some machine tools, and change in load on the table is a common phenomena. In addition, air compressor, vacuum pump, oscilloscope and dynamic signal analyzer with cooling fan rest on the floor. Some more potential energy souces are elevator mechanisms, air conditioning, rail and road transport, heat pumps that contribute to the vibrational background noise and that are coupled to the foundations and floors of the surrounding buildings. All the above sources of vibrations affect the system either directly on the table or transmit from the floor.

## 2.2 Compliance

Compliance is defined as the ratio of the linear or angular displacement to the magnitude of the applied static or constant force. Moreover, in case of a varying dynamic force or vibration, it can be defined as the ratio of the excited vibrational amplitude in any form of angular or translational displacement to the magnitude of the forcing vibration. It is the most extensively used transfer function for the vibrational response of an isolation table. Any deflection of the isolation table is demonstrated by the change in relative position of the components mounted on the table surface. Hence, if the isolation system has virtually zero or lower compliance (infinite stiffness) values, by definition, it is a better-quality table because the deflection of the surface on which fabricated parts are mounted is reduced. Compliance is measured in units of displacement per unit force, i.e., meters/Newton (m/N) and used to measure deflection at different frequencies.

The deformation of a body or structure in response to external payloads or forces is a common problem in engineering fields. These external disturbance forces may be static or dynamic. The development of an isolation table is a good example of this problem where such static and dynamic forces may exist. A static load, such as that caused by a large, concentrated mass loaded or unloaded on the table, can cause the table to deform. A dynamic force, such as the periodic disturbance of a rotating motor placed on top of the table, or vibration induced from the building into the isolation table through its mounting points, can cause the table to oscillate and deform.

Assume the simplest model of conventional mass-spring-damper system as shown in Fig. 1(a), to understand compliance with only one degree-of-freedom system. Consider that a single frequency sinusoidal vibration applied to the system. From Newton's laws, the general equation of motion is given by

$$m\ddot{x} + c\dot{x} + kx = F_0 \sin \omega t, \quad (1)$$

where  $m$  : the mass of the isolated object,  $x$  : the displacement of the mass,  $c$  : the damping,  $k$  : the stiffness,  $F_0$  : the maximum amplitude of the disturbance,  $\omega$  : the rotational frequency of disturbance, and  $t$  : the time.

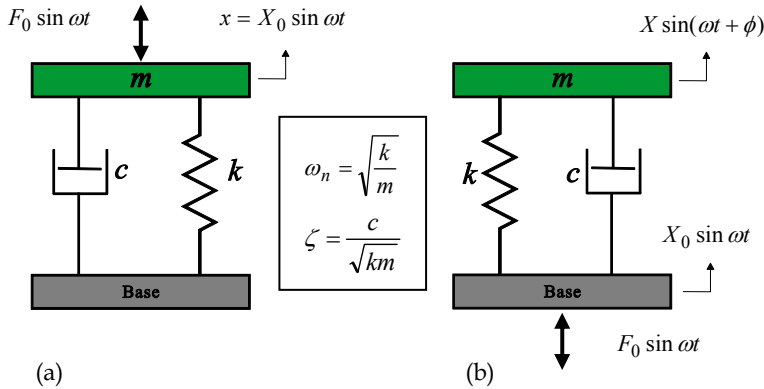


Fig. 1. Conventional mass-spring-damper vibration isolator under (a) direct disturbance (b) ground vibration.

The general expression for compliance of a system presented in Eq. (1) is given by

$$\text{Compliance} = \frac{x}{F} = \frac{1}{\sqrt{(k - m\omega^2)^2 + (c\omega)^2}} \tag{2}$$

The compliance in Eq. (2) can be represented as

$$\text{Compliance} = \frac{x}{F} = \frac{1/k}{\sqrt{(1 - (\omega/\omega_n)^2)^2 + 4\zeta^2(\omega/\omega_n)^2}} \tag{3}$$

where  $\omega_n$  : the natural frequency of the system and  $\zeta$  : the damping ratio.

### 2.3 Transmissibility

Transmissibility is defined as the ratio of the dynamic output to the dynamic input, or in other words, the ratio of the amplitude of the transmitted vibration (or transmitted force) to that of the forcing vibration (or exciting force).

Vibration isolation or elimination of a system is a two-part problem. As discussed in Section 2.1, the tabletop of an isolation system is designed to have zero or minimal response to a disturbing force or vibration. This is itself not sufficient to ensure a vibration free working surface. Typically, the entire table system is subjected continually to vibrational impulses from the laboratory floor. These vibrations may be caused by large machinery within the building as discussed in Section 2.1 or even by wind or traffic-excited building resonances or earthquake.

The model shown in Fig. 1(a) is modified by applying ground vibration, as shown in Fig. 1(b). The absolute transmissibility,  $T$  of the system, in terms of vibrational displacement, is given by

$$\frac{X}{X_0} = \sqrt{\frac{1 + 4\zeta^2(\omega/\omega_n)^2}{(1 - (\omega/\omega_n)^2)^2 + 4\zeta^2(\omega/\omega_n)^2}}. \quad (4a)$$

Similarly, the transmissibility can also be defined in terms of force. It can be defined as the ratio of the amplitude of force transmitted ( $F$ ) to the amplitude of exciting force ( $F_0$ ). Mathematically, the transmissibility in terms of force is given by

$$\frac{F}{F_0} = \sqrt{\frac{1 + 4\zeta^2(\omega/\omega_n)^2}{(1 - (\omega/\omega_n)^2)^2 + 4\zeta^2(\omega/\omega_n)^2}}. \quad (4b)$$

### 3. Zero-Power Controlled Magnetic Levitation

#### 3.1 Magnetic Suspension System

Since last few decades, an active magnetic levitation has been a viable choice for many industrial machines and devices as a non-contact, lubrication-free support (Schweitzer et al., 1994; Kim & Lee, 2006; Schweitzer & Maslen, 2009). It has become an essential machine element from high-speed rotating machines to the development of precision vibration isolation system. Magnetic suspension can be achieved by using electromagnet and/or permanent magnet. Electromagnet or permanent magnet in the magnetic suspension system causes flux to circulate in a magnetic circuit, and magnetic fields can be generated by moving charges or current. The attractive force of an electromagnet,  $F$  can be expressed approximately as (Schweitzer et al., 1994)

$$F = K \frac{I^2}{\delta^2}, \quad (5)$$

where  $K$ : attractive force coefficient for electromagnet,  $I$ : coil current,  $\delta$ : mean gap between electromagnet and the suspended object.

Each variable is given by the sum of a fixed component, which determines its operating point and a variable component, such as

$$I = I_0 + i, \quad (6)$$

$$\delta = D_0 - x, \quad (7)$$

where  $I_0$ : bias current,  $i$ : coil current in the electromagnet,  $D_0$ : nominal gap,  $x$ : displacement of the suspended object from the equilibrium position.

### 3.2 Magnetic Suspension System with Hybrid Magnet

In order to reduce power consumption and continuous power supply, permanent magnets are employed in the suspension system to avoid providing bias current. The suspension system by using hybrid magnet, which consists of electromagnet and permanent magnet is shown in Fig. 2. The permanent magnet is used for the purpose of providing bias flux (Mizuno & Takemori, 2002). This control realizes the steady states in which the electromagnet coil current converges to zero and the attractive force produced by the permanent magnet balances the weight of the suspended object.

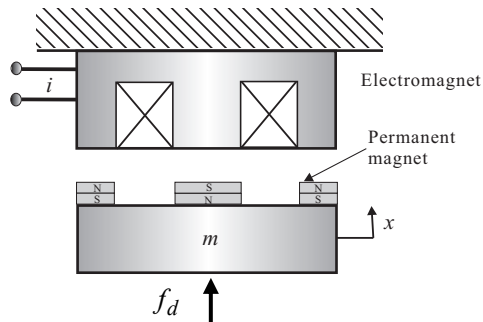


Fig. 2. Model of a zero-power controlled magnetic levitation

It is assumed that the permanent magnet is modeled as a constant-current (bias current) and a constant-gap electromagnet in the magnetic circuit for simplification in the following analysis. Attractive force of the electromagnet,  $F$  can be written as

$$F = K \frac{(I_0 + i)^2}{(D_0 - x)^2}, \quad (8)$$

where bias current,  $I_0$  is modified to equivalent current in the steady state condition provided by the permanent magnet and nominal gap,  $D_0$  is modified to the nominal air gap in the steady state condition including the height of the permanent magnet. Equation (8) can be transformed as

$$F = K \frac{I_0^2}{D_0^2} \left(1 - \frac{x}{D_0}\right)^{-2} \left(1 + \frac{i}{I_0}\right)^2. \quad (9)$$

Using Taylor principle, Eq. (9) can be expanded as

$$F = K \frac{I_0^2}{D_0^2} \left(1 + 2\frac{x}{D_0} + 3\frac{x^2}{D_0^2} + 4\frac{x^3}{D_0^3} + \dots\right) \left(1 + 2\frac{i}{I_0} + \frac{i^2}{I_0^2}\right). \quad (10)$$

For zero-power control system, control current is very small, especially, in the phase approaches to steady-state condition and therefore, the higher-order terms are not considered. Equation (10) can then be written as

$$F = F_e + k_i i + k_s (x + p_2 x^2 + p_3 x^3 + \dots), \quad (11)$$

where

$$F_e = K \frac{I_0^2}{D_0^2}, \quad (12)$$

$$k_i = 2K \frac{I_0}{D_0^2}, \quad (13)$$

$$k_s = 2K \frac{I_0^2}{D_0^3}, \quad (14)$$

$$p_2 = \frac{3}{2D_0}, \quad (15)$$

$$p_3 = \frac{4}{2D_0^2}. \quad (16)$$

For zero-power control system, the control current of the electromagnet is converged to zero to satisfy the following equilibrium condition

$$F_e = mg, \quad (17)$$

and the equation of motion of the suspension system can be written as

$$m\ddot{x} = F - mg. \quad (18)$$

From Eqs. (11), (17) and (18),

$$m\ddot{x} = k_i i + k_s (x + p_2 x^2 + p_3 x^3 + \dots). \quad (19)$$

This is the fundamental equation for describing the motion of the suspended object.

### 3.3 Design of Zero-Power Controller

Negative stiffness is generated by actively controlled zero-power magnetic suspension. The basic model, controller and the characteristic of the zero-power control system is described below.

#### 3.3.1 Model

A basic zero-power controller is designed for simplicity based on linearized equation of motions. It is assumed that the displacement of the suspended mass is very small and the

nonlinear terms are neglected. Hence the linearized motion equation from Eq. (19) can be written as

$$m\ddot{x} = k_i i + k_s x. \tag{20}$$

The suspended object with mass of  $m$  is assumed to move only in the vertical translational direction as shown by Fig. 2. The equation of motion is given by

$$m\ddot{x} = k_s x + k_i i + f_d, \tag{21}$$

where  $x$ : displacement of the suspended object,  $k_s$ : gap-force coefficient of the hybrid magnet,  $k_i$ : current-force coefficient of the hybrid magnet,  $i$ : control current,  $f_d$ : disturbance acting on the suspended object. The coefficients  $k_s$  and  $k_i$  are positive. When each Laplace-transform variable is denoted by its capital, and the initial values are assumed to be zero for simplicity, the transfer function representation of the dynamics described by Eq. (21) becomes

$$X(s) = \frac{1}{s^2 - a_0} (b_0 I(s) + d_0 W(s)), \tag{22}$$

where  $a_0 = k_s / m$ ,  $b_0 = k_i / m$ , and  $d_0 = 1 / m$ .

### 3.3.2 Suspension with Negative Stiffness

Zero-power can be achieved either by feeding back the velocity of the suspended object or by introducing a minor feedback of the integral of current in the PD (proportional-derivative) control system (Mizuno & Takemori, 2002). Since PD control is a fundamental control law in magnetic suspension, zero-power control is realized from PD control in this work using the second approach. In the current controlled magnetic suspension system, PD control can be represented as

$$I(s) = -(p_d + p_v s) X(s), \tag{23}$$

where  $p_d$ : proportional feedback gain,  $p_v$ : derivative feedback gain. Figure 3 shows the block diagram of a current-controlled zero-power controller where a minor integral feedback of current is added to the proportional feedback of displacement.

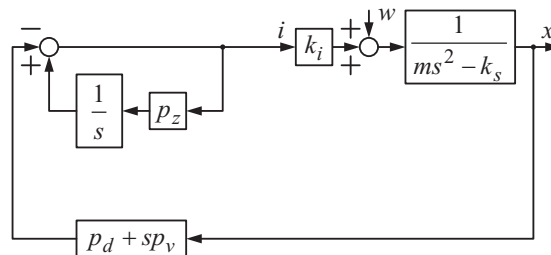


Fig. 3. Transfer function representation of the zero-power controller of the magnetic levitation system



The control current of zero-power controller is given by

$$I(s) = -\left(\frac{s}{s - p_z} p_d + p_v s\right) X(s), \quad (24)$$

where  $p_z$ : integral feedback in the minor current loop. From Eqs. (22) to (24), it can be written as

$$\frac{X(s)}{W(s)} = \frac{(s - p_z)d_0}{s^3 + (b_0 p_v - p_z)s^2 + (b_0 p_d - b_0 p_v p_z - a_0)s + a_0 p_z}, \quad (25)$$

$$\frac{I(s)}{W(s)} = \frac{-s(sp_v + p_d - p_v p_z)d_0}{s^3 + (b_0 p_v - p_z)s^2 + (b_0 p_d - b_0 p_v p_z - a_0)s + a_0 p_z}. \quad (26)$$

To estimate the stiffness for direct disturbance, the direct disturbance,  $W(s)$  on the isolation table is considered to be stepwise, that is

$$W(s) = \frac{F_0}{s}, \quad (F_0 : \text{constant}). \quad (27)$$

The steady displacement of the suspension, from Eqs. (25) and (27), is given by

$$\lim_{t \rightarrow \infty} x(t) = \lim_{s \rightarrow 0} sX(s) = -\frac{d_0}{a_0} F_0 = -\frac{F_0}{k_s}. \quad (28)$$

The negative sign in the right-hand side illustrates that the new equilibrium position is in the direction opposite to the applied force. It means that the system realizes negative stiffness. Assume that stiffness of any suspension is denoted by  $k$ . The stiffness of the zero-power controlled magnetic suspension is, therefore, negative and given by

$$k = -k_s. \quad (29)$$

### 3.3.3 Realization of Zero-Power

From Eqs. (26) and (27)

$$\lim_{t \rightarrow \infty} i(t) = \lim_{s \rightarrow 0} sI(s) = 0. \quad (30)$$

It indicates that control current, all the time, converges to zero in the zero-power control system for any load.

### 3.4 Stiffness Adjustment

The stiffness realized by zero-power control is constant, as shown in Eq. (29). However, it is necessary to adjust the stiffness of the magnetic levitation system in many applications, such as vibration isolation systems. There are two approaches to adjust stiffness of the zero-power control system. The first one is by adding a minor displacement feedback to the zero-power control current, and the other one is by adding a proportional feedback in the minor current feedback loop (Ishino et al., 2009). In this research, stiffness adjustment capability of zero-power control is realized by the first approach. Figure 4 shows the block diagram of the modified zero-power controller that is capable to adjust stiffness. The control current of the modified zero-power controller is given by

$$I'(s) = -\left(\frac{p_d s}{s - p_z} + \frac{p_v s^2}{s - p_z} + p_s\right)X(s), \tag{31}$$

where  $p_s$  : proportional displacement feedback gain across the zero-power controller.

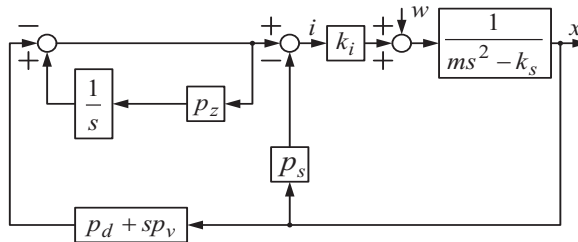


Fig. 4. Block diagram of the modified zero-power controller that can adjust stiffness

The transfer-function representation of the dynamics shown in Fig. 4 is given by

$$\frac{X(s)}{W(s)} = \frac{(s - p_z)d_0}{s^3 + (b_0 p_v - p_z)s^2 + (b_0 p_d + b_0 p_s - a_0)s + a_0 p_z - b_0 p_s p_z}. \tag{32}$$

From Eqs. (27) and (32), the steady displacement becomes

$$\lim_{t \rightarrow \infty} x(t) = \lim_{s \rightarrow 0} sX(s) = -\frac{d_0 p_z}{a_0 p_z - b_0 p_s p_z} F_0 = -\frac{F_0}{k_s - k_i p_s} \tag{33}$$

Therefore, the stiffness of the modified system becomes

$$k = -k_s + k_i p_s. \tag{34}$$

It indicates that the stiffness can be increased or decreased by changing the feedback gain  $p_s$ .

### 3.5 Nonlinear Compensation of Zero-Power Controller

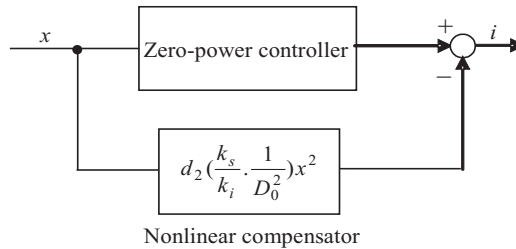


Fig. 5. Block diagram of the nonlinear compensator of the zero-power controlled magnetic levitation

It is shown that the zero-power control can generate negative stiffness. The control current of the zero-power controlled magnetic suspension system is converged to zero for any added mass. To counterbalance the added force due to the mass, the stable position of the suspended object is changed. Due to the air gap change between permanent magnet and the object, the magnetic force is also changed, and hence, the negative stiffness generated by this system varies as well according to the gap (see Eq. (14)). To compensate the nonlinearity of the basic zero-power control system, the first nonlinear terms of Eq. (19) is considered and added to the basic system. From Eq. (19), the control current can be expressed as

$$i = i_{ZP} - d_2 \left( \frac{k_s}{k_i} \cdot \frac{1}{D_0^2} \right) x^2, \tag{35}$$

where  $d_2$  : the nonlinear control gain and,  $i_{zp}$  : the current in the zero-power controller,  $k_s$ ,  $k_i$  and  $D_0$  are constant for the system. The square of the displacement ( $x^2$ ) is fed back to the normal zero-power controller. The block diagram of the nonlinear controller arrangement is shown in Fig. 5. The air gap between the permanent magnet and the suspended object can be changed in order to choose a suitable operating point.

It is worth noting that the nonlinear compensator and the stiffness adjustment controller can be used simultaneously without instability. Moreover, performance of the nonlinear compensation could be improved furthermore if the second and third nonlinear terms and so on are considered together.

## 4. Vibration Suppression Using Zero-Power Controlled Magnetic Levitation

### 4.1 Theory of Vibration Control

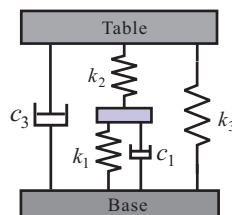


Fig. 6. A model of vibration isolator that can suppress both tabletop and ground vibrations

The vibration isolation system is developed using magnetic levitation technique in such a way that it can behave as a suspension of virtually zero compliance or infinite stiffness for direct disturbing forces and a suspension with low stiffness for floor vibration. Infinite stiffness can be realized by connecting a mechanical spring in series with a magnetic spring that has negative stiffness (Mizuno, 2001; Mizuno et al., 2007a & Hoque et al., 2006). When two springs with spring constants of  $k_1$  and  $k_2$  are connected in series, the total stiffness  $k_c$  is given by

$$k_c = \frac{k_1 k_2}{k_1 + k_2}. \quad (36)$$

The above basic system has been modified by introducing a secondary suspension to avoid some limitations for system design and supporting heavy payloads (Mizuno, et al., 2007a & Hoque, et al., 2010a). The concept is demonstrated in Fig. 6. A passive suspension ( $k_3, c_3$ ) is added in parallel with the serial connection of positive and negative springs. The total stiffness  $\tilde{k}_c$  is given by

$$\tilde{k}_c = \frac{k_1 k_2}{k_1 + k_2} + k_3. \quad (37)$$

However, if one of the springs has negative stiffness that satisfies

$$k_1 = -k_2, \quad (38)$$

the resultant stiffness becomes infinite for both the case in Eqs. (36) and (37) for any finite value of  $k_3$ , that is

$$|\tilde{k}_c| = \infty. \quad (39)$$

Equation (39) shows that the system may have infinite stiffness against direct disturbance to the system. Therefore, the system in Fig. 6 shows virtually zero compliance when Eq. (38) is satisfied. On the other hand, if low stiffness of mechanical springs for system ( $k_1, k_3$ ) are used, it can maintain good ground vibration isolation performance as well.

#### 4.2 Typical Applications of Vibration Suppression

In this section, typical vibration isolation systems using zero-power controlled magnetic levitation are presented, which were developed based on the principle discussed in Eq. (37). The isolation system consists mainly of two suspensions with three platforms- base, middle table and isolation table. The lower suspension between base and middle table is of positive stiffness and the upper suspension between middle table and base is of negative stiffness realized by zero-power control. A passive suspension directly between base and isolation table acts as weight support mechanism.

A typical single-axis and a typical six-axis vibration isolation apparatuses are demonstrated in Fig. 7. The single-axis apparatus (Fig. 7(a)) consisted of a circular base, a circular middle table and a circular isolation table. The height, diameter and weight of the system were 300mm, 200mm and 20 kg, respectively. The positive stiffness in the lower part was realized by three mechanical springs and an electromagnet. To reduce coil current in the electromagnet, four permanent magnets (15mm×2mm) were used. The permanent magnets are made of Neodymium-Iron-Boron (NdFeB). The stiffness of each coil springs was 3.9

N/mm. The electromagnet coil had 180-turns and  $1.3\Omega$  resistance. The wire diameter of the coil was 0.6 mm. The relative displacement of the base to middle table was measured by an eddy-current displacement sensor, provided by Swiss-made Baumer electric. The negative stiffness suspension in the upper part was achieved by a hybrid magnet consisted of an electromagnet that was fixed to the middle table, and six permanent magnets attached to the electromagnet target on the isolation table. Another displacement sensor was used to measure the relative displacement between middle table to isolation table. The isolation table was also supported by three coil springs as weight support mechanism, and the stiffness of the each spring was 2.35 N/mm.

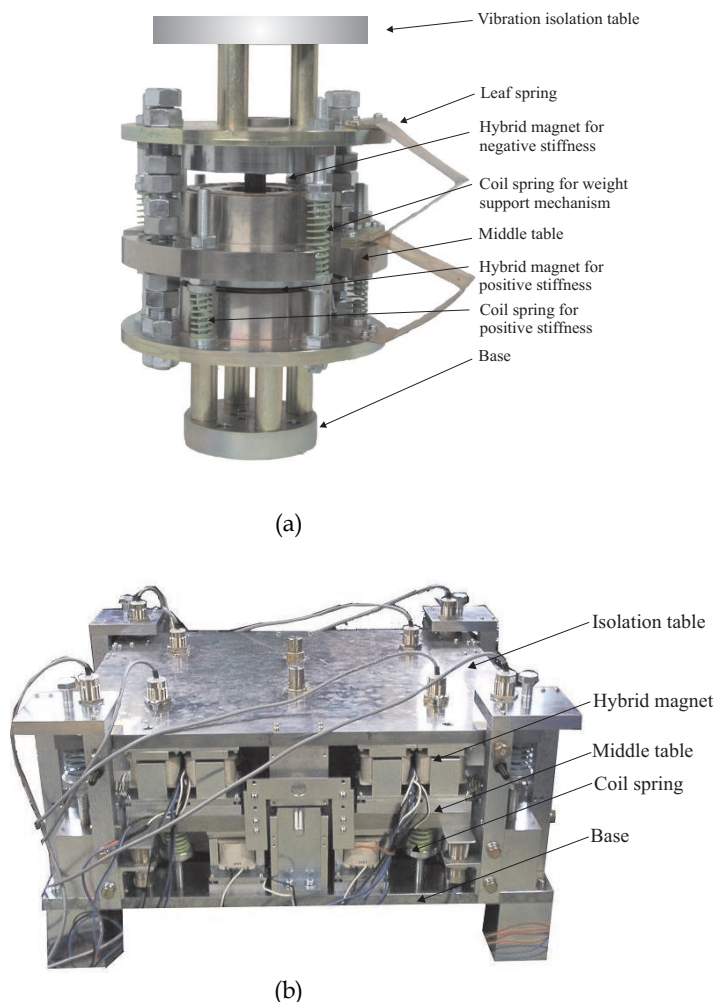


Fig. 7. Typical applications of zero-power controlled magnetic levitation for active vibration control (a) single-degree-of-freedom system (b) six-degree-of-freedom system

The six-axis vibration isolation system with magnetic levitation technology is shown in Fig. 7(b) (Hoque, et al., 2010a). It consisted of a rectangular isolation table, a middle table and base. A positive stiffness suspension realized by electromagnet and normal springs was used between the base and the middle table. On the other hand, a negative stiffness suspension generated by hybrid magnets was used between the middle table and the isolation table. The height, length, width and mass of the apparatus were 300 mm, 740 mm, 590 mm and 400 kg, respectively. The isolation and middle tables weighed 88 kg and 158 kg, respectively. The isolation table had six-degree-of-freedom motions in the  $x$ ,  $y$ ,  $z$ , roll, pitch and yaw directions.

The base was equipped with four pairs of coil springs and electromagnets to support the middle table in the vertical direction and six pairs of coil springs and electromagnets (two pairs in the  $x$ -direction and four pairs in the  $y$ -direction) in the horizontal directions. The middle table was equipped with four sets of hybrid magnets to levitate and control the motions of the isolation table in the vertical direction and six sets of hybrid magnets (two sets in the  $x$ -direction and four sets in the  $y$ -direction) to control the motions of the table in the horizontal directions. The isolation table was also supported by four coil springs in the vertical direction and six coil springs (two in the  $x$ -direction and four in the  $y$ -direction) in the horizontal directions as weight support mechanism. Each set of hybrid magnet for zero-power suspension consisted of five square-shaped permanent magnets (20 mm×20 mm×2 mm) and five 585-turn electromagnets. The spring constant of each normal spring was 12.1 N/mm and that of weight support spring was 25.5 N/mm. There was flexibility to change the position of the weight support springs both in the vertical and horizontal directions to make it compatible for designing stable magnetic suspension system using zero-power control. The relative displacements of the isolation table to the middle table and those of the middle table to the base were detected by eight eddy-current displacement sensors attached to the corners of the isolation table and the base.

A DSP-based digital controller (DS1103) was used for the implementation of the designed control algorithms by simulink in Matlab. The sampling rate was 10 kHz.

### 4.3 Experimental Demonstrations

Several experiments have been conducted to verify the aforesaid theoretical analysis. The nonlinear compensation of zero-power controlled magnetic levitation, stiffness adjustment of the levitation system are confirmed initially. Then the characteristics of the developed isolation systems are measured in terms of compliance and transmissibility.

#### 4.3.1 Nonlinear Compensation of Magnetic Levitation System

First of all, zero-power control was realized between the isolation table and the middle table for stable levitation. Static characteristic of the zero-power controlled magnetic levitation was measured as shown in Fig. 8 when the payloads were increased to produce static direct disturbances on the table in the vertical direction.

In this case, the middle table was fixed and the table was levitated by zero-power control. The result presents the load-stiffness characteristic of the zero-power control system. The figure without nonlinear compensation indicates that there was a wide variation of stiffness when the downward load force changed. For the uniform load increment, the change of gap was not equal due to the nonlinear magnetic force. Therefore, the negative stiffness generated from zero-power control was nonlinear which may severely affect the vibration isolation system.

To overcome the above problem, the nonlinear compensator was introduced in parallel with the zero-power control system. The nonlinear control gain ( $d_2$ ) was chosen by trial and error method. The gap ( $D_0$ ) between the table and the electromagnet was 5.1 mm after stable levitation by zero-power control. The value of  $k_s$  and  $k_i$  were determined from the system characteristics. The load-stiffness characteristic using nonlinear compensation is also shown in the figure. It is obvious from the figure that the linearity error was reduced when control gain ( $d_2$ ) was increased. For  $d_2 = 55$ , the linearity error was very low and the stiffness generated from the system was approximately constant. This result shows the potential to improve the static response performance of the isolation table to direct disturbance.

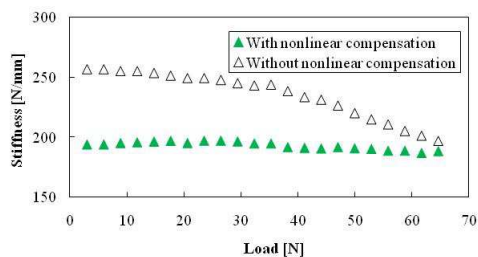


Fig. 8. Nonlinear compensation of the conventional zero-power controlled magnetic levitation system

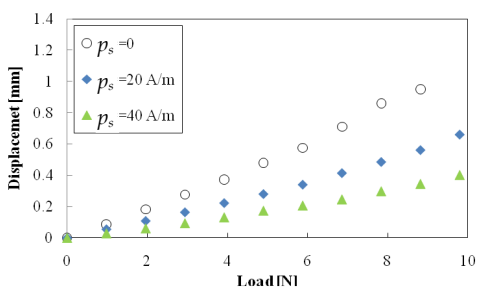


Fig. 9. Load-displacement characteristics of the modified zero-power controlled magnetic levitation system

#### 4.3.2 Stiffness Adjustment of Zero-Power Controlled Magnetic Levitation

The experiments have been carried out to measure the performances of the modified zero-power controller. Figure 9 shows the load-displacement characteristics of the system with the improved zero-power controller (Fig. 4). When the proportional feedback gain,  $p_s = 0$ , it can be considered as a conventional zero-power controller (Fig. 3). The result shows that when the payloads were put on the suspended object, the table moved in the direction opposite to the applied load, and the gap was widened. It indicates that the zero-power control realized negative displacement, and hence its stiffness is negative, as described by Eqs. (28) and (29). The conventional zero-power controller ( $p_s = 0$ ) realized fixed negative stiffness of magnitude  $-9.2$  N/mm. When the proportional feedback gain,  $p_s$  was changed, the stiffness also gradually increased. When  $p_s = 40$  A/m, negative stiffness was increased to  $-21.5$  N/mm. It confirms that proportional feedback gain,  $p_s$  can change the stiffness of the zero-power controller, as explained in Eq. (34).

#### 4.3.3 Experimental Results with Vibration Isolation System

Further experiments were conducted with the linearized zero-power controller with the vibration isolation system, as shown in Fig. 10. In this case, the positive and negative stiffness springs were, then, adjusted to satisfy Eq. (38). The stiffness could either be adjusted in the positive or negative stiffness part. In the former, PD control could be used in the electromagnets that were employed in parallel with the coil springs. The latter technique was presented in Section 4.3.2. For better performance, the latter was adopted in this work.

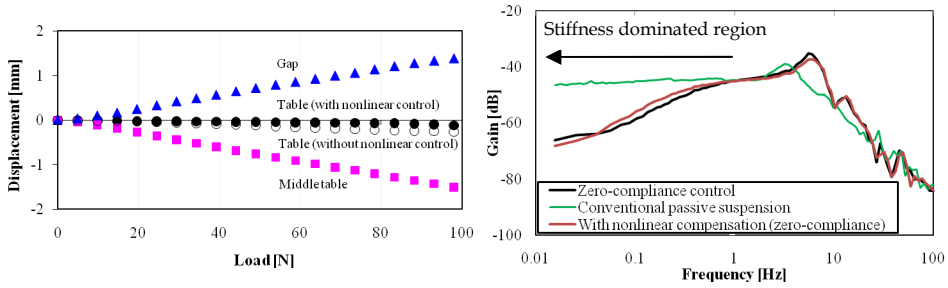


Fig. 10. Static characteristics of the isolation table with and without nonlinear control

Fig. 11. Dynamic characteristics of the isolation table in the vertical direction

Figure 10 demonstrates the performance improvement of the controller for static response to direct disturbance. The displacements of the isolation table and middle table were plotted against disturbing forces produced by payload in the vertical direction. It is clear that zero-compliance to direct disturbance was realized up to 100 N payloads with nonlinear controller ( $d_2=55$ ). The stiffness of the isolation system was increased to 960 N/mm which was approximately 2.8 times more than that of without nonlinear control. The figure illustrates significant improvement in rejecting on-board-generated disturbances.

The dynamic performance of the isolation table was measured in the vertical direction as shown in Fig. 11. In this case, the isolation table was excited to produce sinusoidal disturbance force by two voice coil motors which were attached to the base and can generate force in the Z-direction. The displacement of the table was measured by gap sensors and the data was captured by a dynamic signal analyzer. It is found from the figure that high stiffness, that means virtually zero-compliance, was realized at low frequency region (-66 dB[mm/N] at 0.015 Hz). It also demonstrates that direct disturbance rejection performance was not worsened even nonlinear zero-power control was introduced.

Finally a comparative study of the disturbance suppression performance was conducted with zero-compliance control and conventional passive suspension technique as shown in the figure. The experiment was carried out with same lower suspension for ground vibration isolation. First, the isolation table was suspended by positive suspension (conventional spring-damper) and frequency response to direct disturbance was measured. The stiffness dominated region is marked in the figure, and it is seen from the figure that the displacement of the isolation table was almost same below 1 Hz (approximately -46 dB). However, when the isolation table was suspended by zero-compliance control satisfying Eqs. (38) and (39), displacement of the table was abruptly reduced at the low frequency region below 1 Hz (-66 dB at 0.015 Hz). It is confirmed from the figure that the developed zero-compliance system had better direct disturbance rejection performance over the conventional passive suspension even both the systems used similar vibration isolation performances.



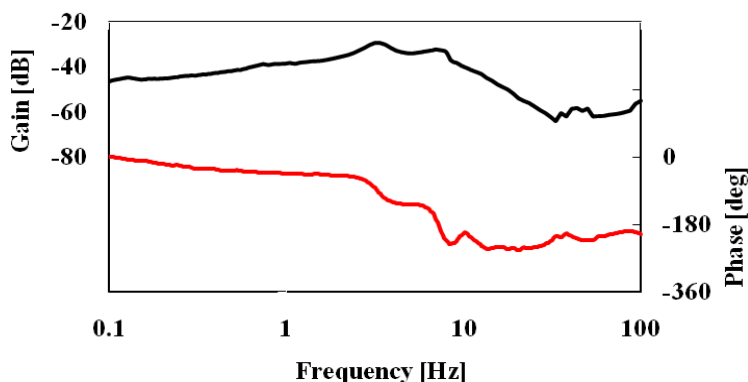


Fig. 12. Dynamic characteristics of the isolation table in the vertical direction.

The characteristics of the isolation table were further investigated by measuring the response of the table to direct disturbance in the horizontal directions as shown in Fig. 12. In this case, four voice coil motors were used to excite the isolation table along the horizontal direction. The results show the dynamic response of the isolation table when the table was excited along yaw mode. The response of the table to direct dynamic disturbance was captured by dynamic signal analyzer. The results justify that the displacements of the table to direct disturbance in the horizontal rotational motions were also low at the low frequency regions. The results confirmed that the isolation table was realized high stiffness against disturbing forces in the motion associated with horizontal direction.

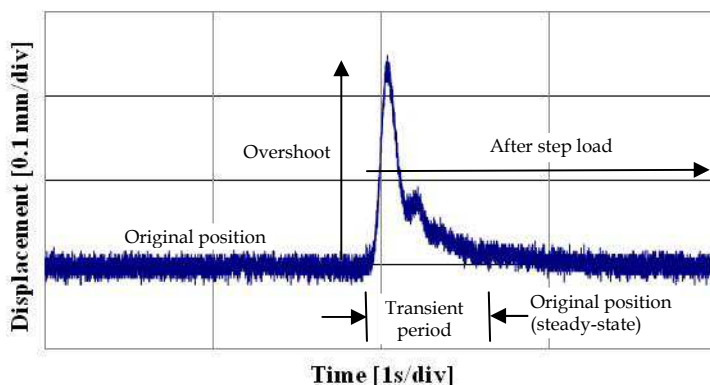


Fig. 13. Step response of the isolation table with magnetic levitation technology

The step response of the isolation table is shown in Fig. 13. In this experiment, a stepwise disturbance was generated by suddenly removing a certain amount of load from the table and the response was measured. The results showed that the table moved upward in the direction of load removal and returned to the original position (steady-state) after certain period. However, there was a reverse action in case of step wise disturbance. Therefore, a

peak was appeared due to the response of the step load. This unpleasant response might hamper the objective function of many advanced systems. It can be noted that a feedforward controller can be added in combination with zero-power control to overcome this problem.

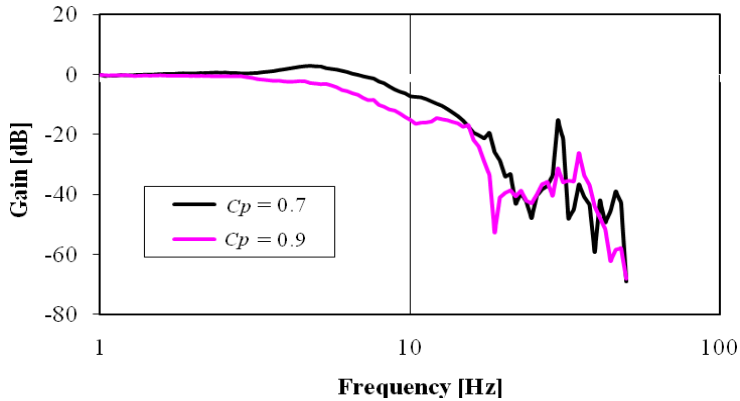


Fig. 14. Transmissibility characteristics of the isolation table.

Figure 14 shows the absolute transmissibility of the isolation table from the base of the developed system. In this case, the base of the system was sinusoidally excited in the vertical direction by a high-powered pneumatic actuator attached to the base, and the displacement transfer function (transmissibility) of the isolation table was measured from the base. The base displacement in the vertical direction was considered as input, and the output signal was the displacement of the isolation table. The damping coefficient ( $c_p$ ) between the base and the middle table played important role to suppress the resonance peak. The figure shows that the resonant peak was almost suppressed when  $c_p$  was chosen as 0.9. It is clear from the figure that the developed system can effectively isolate the floor vibration that transmitted through the suspensions, such as active-passive positive suspensions and active zero-power controlled magnetic levitation.

## 5. Conclusions

A zero-power controlled magnetic levitation system has been presented in this chapter. The unique characteristic of the zero-power control system is that it can generate negative stiffness with zero control current in the steady-state which is realized in this chapter. The detail characteristics of the levitation system are investigated. Moreover, two major contributions, the stiffness adjustment and nonlinear compensation of the suspension system have been introduced elaborately. Often, there is a challenge for the vibration isolator designer to tackle both direct disturbance and ground vibration simultaneously with minimum system development and maintenance costs. Taking account of the point of view, typical applications of active vibration isolation using zero-power controlled magnetic levitation has been presented. The vibration isolation system is capable to suppress the effect of tabletop vibration as well as to isolate ground vibration. Some experimental demonstrations are presented that verifies the feasibility of its application in many industries and space related instruments. Moreover, it can be noted that a feedforward controller in combination with the zero-power controller can be used to improve the performance of the isolator to suppress direct disturbances.

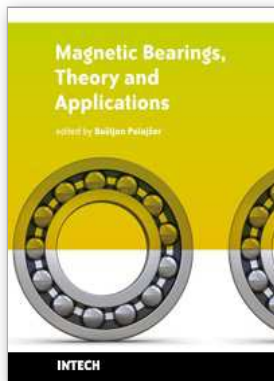
## 6. Acknowledgment

The authors gratefully acknowledge the financial support made available from the Japan Society for the Promotion of Science as a Grant-in-Aid for scientific research (Grant no. 20.08380) for the foreign researchers and the Ministry of Education, Culture, Sports, Science and Technology of Japan, as a Grant-in-Aid for Scientific Research (B).

## 7. References

- Benassi, L. ; Elliot, S. J. & Gardonio, P. (2004a). Active vibration isolation using an inertial actuator with local force feedback control, *Journal of Sound and Vibration*, Vol. 276, No. 3, pp. 157-179
- Benassi, L. & Elliot, S. J. (2004b). Active vibration isolation using an inertial actuator with local displacement feedback control, *Journal of Sound and Vibration*, Vol. 278, No. 4-5, pp. 705-724
- Daley, S. ; Hatonen, J. & Owens, D. H. (2006). Active vibration isolation in a "smart spring" mount using a repetitive control approach, *Control Engineering Practice*, Vol. 14, pp. 991-997.
- Fuller, C. R. ; Elliott, S. J. & Nelson, P. A. (1997). *Active Control of Vibration*, Academic Press, ISBN 0-12-269440-6, New York, USA
- Harris, C. M. & Piersol, A. G. (2002). *Shock and Vibration Handbook*, McGraw Hill, Fifth Ed., ISBN 0-07-137081-1, New York, USA
- Hoque, M. E. ; Takasaki, M. ; Ishino, Y. & Mizuno, T. (2006). Development of a three-axis active vibration isolator using zero-power control, *IEEE/ASME Transactions on Mechatronics*, Vol. 11, No. 4, pp. 462-470
- Hoque, M. E. ; Mizuno, T. ; Ishino, Y. & Takasaki, M. (2010a). A six-axis hybrid vibration isolation system using active zero-power control supported by passive support mechanism, *Journal of Sound and Vibration*, Vol. 329, No. 17, pp. 3417-3430
- Hoque, M. E. ; Mizuno, T. ; Kishita, D. ; Takasaki, M. & Ishino, Y. (2010b). Development of an Active Vibration Isolation System Using Linearized Zero-Power Control with Weight Support Springs, *ASME Journal of Vibration and Acoustics*, Vol. 132, No. 4, pp. 041006-1/9
- Ishino, Y. ; Mizuno, T. & Takasaki, M. (2009). Stiffness Control of Magnetic Suspension by Local Feedback, Proceedings of the European Control Conference 2009, pp. 3881-3886, Budapest, Hungary, 23-26 August, 2009
- Karnopp, D. (1995). Active and semi-active vibration isolation, *ASME Journal of Mechanical Design*, Vol. 117, pp. 177-185
- Kim, H. Y. & Lee, C. W. (2006). Design and control of Active Magnetic Bearing System With Lorentz Force-Type Axial Actuator, *Mechatronics*, vol. 16, pp. 13-20
- Mizuno, T. (2001). Proposal of a Vibration Isolation System Using Zero-Power Magnetic Suspension, Proceedings of the Asia Pacific Vibration Conference 2001, pp. 423-427, Hangzhou, China
- Mizuno, T. & Takemori, Y. (2002). A transfer-function approach to the analysis and design of zero-power controllers for magnetic suspension system, *Electrical Engineering in Japan*, Vol. 141, No. 2, pp. 933-940
- Mizuno, T. ; Takasaki, M. ; Kishita, D. & Hirakawa, K. (2007a). Vibration isolation system combining zero-power magnetic suspension with springs, *Control Engineering Practice*, Vol. 15, No. 2, pp. 187-196
- Mizuno, T. ; Furushima, T. ; Ishino, Y. & Takasaki, M. (2007b). General Forms of Controller Realizing Negative Stiffness, Proceedings of the SICE Annual Conference 2007, pp. 2995-3000, Kagawa University, Japan, 17-20 September, 2007

- Morishita, M. ; Azukizawa, T. ; Kanda, S. ; Tamura, N. & Yokoyama, T. (1989). A new maglev system for magnetically levitated carrier system, *IEEE Transaction on Vehicular Technology*, Vol. 38, No. 4, pp. 230-236
- Platus, D. L. (1991). Negative-stiffness-mechanism vibration isolation system, Proceedings of the SPIE, *Vibration Control in Microelectronics, Optics, and Metrology*, Vol. 1619, pp. 44-54
- Preumont, A. (2002). *Vibration Control of Active Structures, An Introduction*, Kluwer, Second ed., ISBN 1-4020-0496-6, Dordrecht
- Preumont, A. ; Francois, A. ; Bossens, F. & Hanieh, A. A. (2002). Force feedback versus acceleration feedback in active vibration isolation, *Journal of Sound and Vibration*, Vol. 257, No. 4, pp. 605-613
- Rivin, E. I. (2003). *Passive Vibration Isolation*, ASME Press, ISBN: 0-7918-0187-X, New York, USA
- Sabnis, A. V. ; Dendy, J. B. & Schmitt, F. M. (1975). Magnetically suspended large momentum wheel, *Journal of Spacecraft and Rockets*, Vol. 12, pp. 420-427
- Sato, T. & Trumper, D. L. (2002). A novel single degree-of-freedom active vibration isolation system, Proceedings of the 8th International Symposium on Magnetic Bearing, pp. 193-198, Japan, August 26-28, 2002
- Schweitzer, G. ; Bleuler, H. & Traxler, A. (1994). *Active Magnetic Bearings*, vdf Hochschulverlag AG an der ETH Zurich, Zurich, Switzerland
- Schweitzer, G. & Maslen, E. H. (2009). *Magnetic Bearings- Theory, Design, and Application to Rotating Machinery*, ISBN : 978-3-642-00496-4, Springer, Germany
- Yoshioka, H. ; Takahashi, Y. ; Katayama, K. ; Imazawa, T. & Murai, N. (2001). An active microvibration isolation system for hi-tech manufacturing facilities, *ASME Journal of Vibration and Acoustics*, Vol. 123, pp. 269-275
- Zhu, W. H. ; Tryggvason, B. & Piedboeuf, J. C. (2006). On active acceleration control of vibration isolation systems, *Control Engineering Practice*, Vol. 14, No. 8, pp. 863-873



## **Magnetic Bearings, Theory and Applications**

Edited by Bostjan Polajzer

ISBN 978-953-307-148-0

Hard cover, 132 pages

**Publisher** Sciyo

**Published online** 06, October, 2010

**Published in print edition** October, 2010

The term magnetic bearings refers to devices that provide stable suspension of a rotor. Because of the contact-less motion of the rotor, magnetic bearings offer many advantages for various applications. Commercial applications include compressors, centrifuges, high-speed turbines, energy-storage flywheels, high-precision machine tools, etc. Magnetic bearings are a typical mechatronic product. Thus, a great deal of knowledge is necessary for its design, construction and operation. This book is a collection of writings on magnetic bearings, presented in fragments and divided into six chapters. Hopefully, this book will provide not only an introduction but also a number of key aspects of magnetic bearings theory and applications. Last but not least, the presented content is free, which is of great importance, especially for young researcher and engineers in the field.

### **How to reference**

In order to correctly reference this scholarly work, feel free to copy and paste the following:

Emdadul Hoque and Takeshi Mizuno (2010). Magnetic Levitation Technique for Active Vibration Control, Magnetic Bearings, Theory and Applications, Bostjan Polajzer (Ed.), ISBN: 978-953-307-148-0, InTech, Available from: <http://www.intechopen.com/books/magnetic-bearings--theory-and-applications/magnetic-levitation-technique-for-active-vibration-control>

# **INTECH**

open science | open minds

### **InTech Europe**

University Campus STeP Ri  
Slavka Krautzeka 83/A  
51000 Rijeka, Croatia  
Phone: +385 (51) 770 447  
Fax: +385 (51) 686 166  
[www.intechopen.com](http://www.intechopen.com)

### **InTech China**

Unit 405, Office Block, Hotel Equatorial Shanghai  
No.65, Yan An Road (West), Shanghai, 200040, China  
中国上海市延安西路65号上海国际贵都大饭店办公楼405单元  
Phone: +86-21-62489820  
Fax: +86-21-62489821

© 2010 The Author(s). Licensee IntechOpen. This chapter is distributed under the terms of the [Creative Commons Attribution-NonCommercial-ShareAlike-3.0 License](#), which permits use, distribution and reproduction for non-commercial purposes, provided the original is properly cited and derivative works building on this content are distributed under the same license.